Identification of ceRNA-vsiRNA-mRNA network for exploring the mechanism underlying pathogenesis of sugarcane mosaic virus in resistant and susceptible maize inbred lines

Xinran Gao[1†], Kaiqiang Hao[1†], Zhichao Du[1], Sijia Zhang[1], Zhiping Wang[1], Mengnan An[1], Zihao Xia[1*] and Yuanhua Wu[1*]

Abstract

RNA silencing plays an important role in plant antiviral responses, which trigger the production of virus-derived small interfering RNAs (vsiRNAs). The competing endogenous RNA (ceRNA) hypothesis revealed a unique mechanism in which circular RNAs (circRNAs) and long non-coding RNAs (lncRNAs) can interact with small RNAs to regulate the expression of corresponding target mRNAs. Sugarcane mosaic virus (SCMV) infection causes severe economic losses in maize (*Zea mays* L.) production worldwide. This study compared and analyzed characteristics of vsiR-NAs derived from SCMV and their target genes in resistant (Chang7-2) and susceptible (Mo17) maize inbred lines through whole-transcriptome RNA sequencing and degradome sequencing. The results showed that 706 transcripts were targeted by 204 vsiRNAs, including 784 vsiRNA-target gene pairs. Furthermore, ceRNA networks of circRNA/lncRNA-vsiRNA-mRNA in response of maize to SCMV infection were obtained, including 3 differentially expressed (DE) circRNAs, 36 DElncRNAs, 105 vsiRNAs, and 342 DEmRNAs in Mo17 plants, and 3 DEcircRNAs, 35 DElncRNAs, 23 vsiRNAs, and 87 DEmRNAs in Chang7-2 plants. Our results also showed that the transcripts of *ZmDCLs*, *ZmAGOs*, and *ZmRDRs* were differentially accumulated in resistant and susceptible maize inbred lines after SCMV infection. These findings provide valuable insights into the relationship between SCMV-derived vsiRNAs and potential ceRNAs fine-tuning the SCMV-maize interaction and offer novel clues to reveal the mechanism underlying the pathogenesis of SCMV.

Keywords Sugarcane mosaic virus (SCMV), vsiRNAs, ceRNA, Maize, Inbred lines

†Xinran Gao and Kaiqiang Hao equally contributed to this work.

*Correspondence:
Zihao Xia
zihao8337@syau.edu.cn
Yuanhua Wu
wuyh09@syau.edu.cn
[1] Liaoning Key Laboratory of Plant Pathology, College of Plant Protection, Shenyang Agricultural University, Shenyang 110866, China

Background

Maize (*Zea mays* L.) is an essential crop for human food, animal feed, and industrial material, which is also a classic model plant for genetics research (Gore et al. 2009). Sugarcane mosaic virus (SCMV) is a positive-sense single-stranded RNA (+ ssRNA) virus in the genus *Potyvirus* of the family *Potyviridae*. SCMV can infect maize, sorghum (*Sorghum vulgare*), sugarcane (*Saccharum sinensis*), and many other Gramineae crops, causing significant losses in various field crops worldwide (Shi et al. 2005).

Gao *et al. Phytopathology Research*   (2023) 5:60

Page 2 of 18

SCMV is the primary causal agent of maize dwarf mosaic disease in China, which initially causes chlorotic symptoms at the base of the leaf and then extends to the whole leaf until a stripe mosaic pattern appears on maize (Jiang and Zhou 2002). Breeding and planting resistant maize varieties are the most economical and effective methods to control SCMV infection. Therefore, exploring the interaction between SCMV and maize plants is important for developing effective virus-control strategies and cultivating disease-resistant varieties.

RNA silencing is a natural antiviral mechanism in plants, which is triggered by double-stranded RNAs (dsRNAs) with different sources and lengths (Pumplin and Voinnet 2013). Plant Dicer-like (DCL) and Argonaute (AGO) proteins play crucial antiviral roles in the RNA silencing pathway (Bouché et al. 2006; Schuck et al. 2013). The dsRNAs are cleaved by DCL proteins into virus-derived small interfering RNAs (vsiRNAs) of 21 to 24 nucleotides (nt) (Ding and Voinnet 2007). Previous studies have shown that plants infected with positive-strand RNA viruses mainly generate 21-nt vsiR-NAs processed by DCL4, while 22-nt vsiRNAs produced by DCL2 are accumulated when the activity of DCL4 is reduced or inhibited (Bouché et al. 2006; Ding 2010). DCL1 and DCL3 can produce 21- and 24-nt vsiRNAs in *dcl2/dcl3/dcl4* and *dcl2/dcl4* mutant plants, respectively (Bouché et al. 2006; Qu et al. 2008). The vsiRNAs are loaded into RNA-induced silencing complexes (RISCs), which contain Argonaute (AGO) proteins, guiding the degradation of viral RNAs and host target mRNAs in a sequence-specific manner (Baumberger and Baulcombe 2005). In *Arabidopsis*, AGOs 1, 2, 4, 5, 7, and 10 can bind vsiRNAs upon different virus infections (Carbonell and Carrington 2015). AGO1 is most important in plant antiviral defense (Harvey et al. 2011). Moreover, AGO2 can protect against suppressor-defective tomato bushy stunt virus (TBSV) in *Nicotiana benthamiana* (Scholthof et al. 2011). AGO4 also shows antiviral function in CMV-infected *N. benthamiana* (Ye et al. 2009). AGO1 and AGO18 are the main antiviral AGOs against rice stripe virus (RSV) and rice dwarf virus (RDV) in rice (Carbonell and Carrington 2015). In plants, the effect of RNA silencing can be amplified by cellular RNA-dependent RNA polymerases (RDRs), which synthesize dsRNAs and produce secondary vsiRNAs (Wang et al. 2010).

Previous studies have shown that vsiRNAs are mainly responsible for RNA silencing mediated antiviral immunity (Zhu et al. 2011). Recently, more and more studies suggest that vsiRNAs play potential regulatory roles in the expression of host genes, which determines the manifestation of viral symptoms in host plants (Wang et al. 2022). The first report of this phenomenon was the vsiRNAs derived from CMV Y-satellite that specifically regulate the expression of chlorophyll-related gene (*ChlI*) and modulate the typical yellowing symptoms in *N. benthamiana* (Smith et al. 2011; Shimura et al. 2011). It has also been reported that Chinese wheat mosaic virus (CWMV) RNA1-derived vsiRNA-20 can cleave the mRNA of *TaVP* to maintain a weak alkaline environment in the cytoplasm to enhance CWMV infection in wheat (Yang et al. 2020; Huang et al. 2022).

Recently, competing endogenous RNAs (ceRNAs) have been widely accepted as a new mode of gene regulation, of which circular RNAs (circRNAs) and long non-coding RNAs (lncRNAs) can act as ceRNAs to regulate miRNA or vsiRNA activity (Song et al. 2021). Based on this mechanism, many studies have analyzed the regulatory network of ceRNA-miRNA/siRNA-target gene in plants (Salmena et al. 2011). For example, maize lncRNA *PILNCR1* inhibits miR399-guided cleavage of *PHOSPHATE2* (*PHO2*) to regulate plant tolerance to low phosphate (Du et al. 2018). Tomato lncRNA08489-miR482e module was reported to enhance host resistance to *Phytophthora infestans* through the reactive oxygen species (ROS)-scavenging system (Liu et al. 2022). In addition, *LINC-AP2* contributes to the formation of shorter stamen in the flowers of *A. thaliana* plants infected with turnip crinkle virus (TCV) by anti-cis downregulating the expression of *AP2* gene (Gao et al. 2016). Tomato lncRNA *SlLNR1* interacts with vsiRNAs derived from a non-coding intergenic region (IR) of tomato yellow leaf curl virus (TYLCV) and suppresses disease development during viral infection (Yang et al. 2019). However, there is still a lack of comprehensive research on the interactions among circRNA, lncRNA, vsiRNA, and mRNA in virus-infected maize plants.

Our previous studies have reported the vsiRNA expression profiles in SCMV-infected maize inbred lines Zong 31 and B73 plants (Xia et al. 2014, 2016). The construction of ceRNA-vsiRNA-mRNA networks of susceptible and resistant plants is beneficial for analyzing the pathogenic mechanism of SCMV and the antiviral responses of host plants. In this study, whole-transcriptome RNA sequencing and degradome sequencing were performed on Chang7-2 (resistant) and Mo17 (susceptible) with or without SCMV infection to compare and identify the critical ceRNA-vsiRNA-mRNA modules, aiming to establish a vsiRNA-mediated regulatory network associated with pathogenesis of SCMV and viral disease resistance in maize.

Results

Symptoms and viral accumulations in SCMV-infected Mo17 and Chang7-2 maize plants

To explore the pathogenicity of SCMV on maize, the resistant (Chang7-2) and susceptible (Mo17) inbred
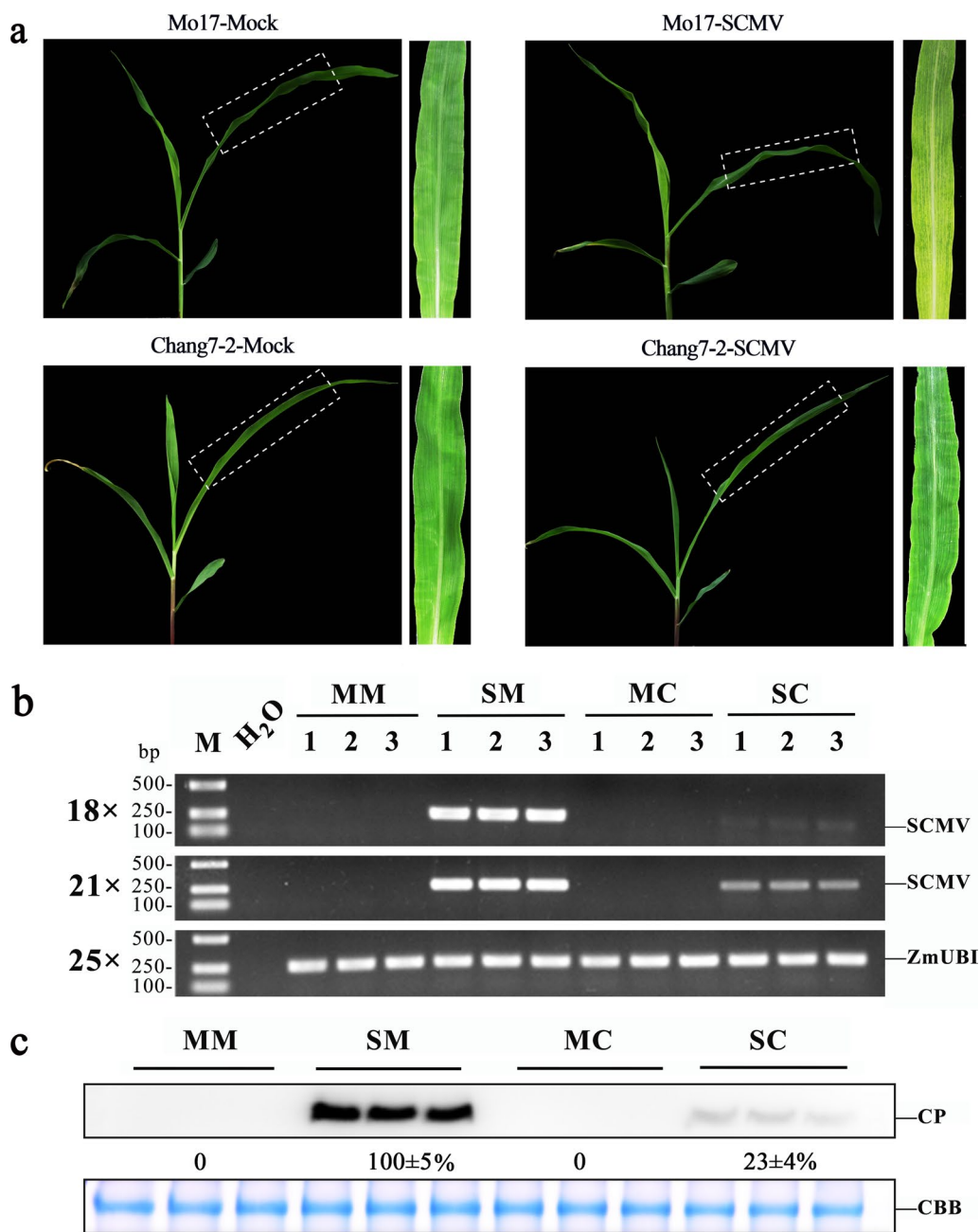
Fig. 1 The symptoms and viral accumulations in SCMV-infected Chang7-2 and Mo17 maize plants. **a** The symptoms on Mo17 and Chang7-2 maize plants inoculated by SCMV or phosphate buffer (Mock) at 10 dpi. **b** The accumulation of SCMV RNA at 10 dpi in Mo17 and Chang7-2 maize plants determined by semiquantitative RT-PCR. 18×, 21×, and 25× indicate cycle numbers in semiquantitative RT-PCR reaction. M: Marker. ZmUBI, internal control. **c** SCMV coat protein (CP) levels at 10 dpi in Mo17 and Chang7-2 maize plants determined by western blot. CBB, Coomassie brilliant blue. MM, Mo17 inoculated with phosphate buffer; SM, Mo17 inoculated with SCMV; MC, Chang7-2 inoculated with phosphate buffer; SC, Chang7-2 inoculated with SCMV

lines were inoculated with SCMV and the phosphate buffer (Mock). At 10 days post inoculation (dpi), systemically infected leaves of Mo17 showed obvious mosaic symptoms, while those of Chang7-2 showed no symptoms (Fig. 1a). The results of semiquantitative reverse transcription-polymerase chain reaction (RT-PCR) and western blot assays showed that the accumulations of SCMV genomic RNA and coat protein (CP) in Mo17 were much higher than that in Chang7-2 (Fig. 1b, c).
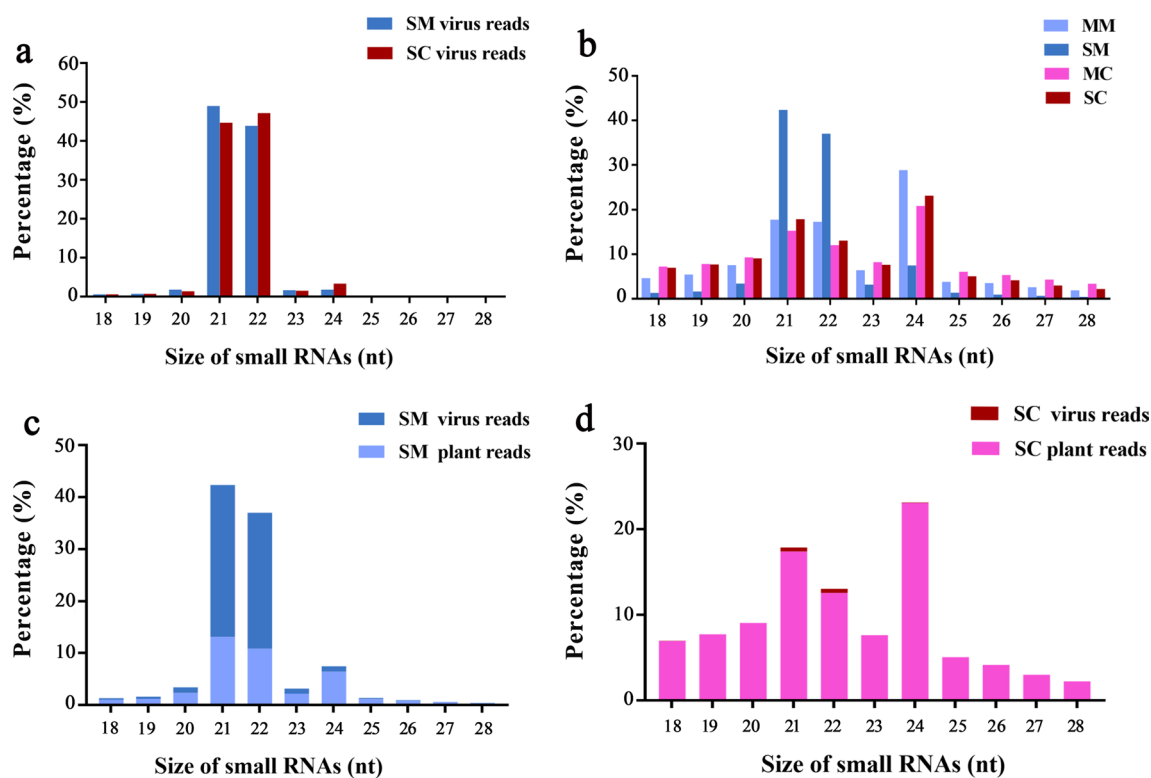
Fig. 2 Accumulation of vsiRNAs in Mo17 and Chang7-2 after SCMV infection. **a** Size distribution of total vsiRNAs in SM and SC libraries. **b** Size distribution of total small RNAs in different libraries. **c** Size distribution of total small RNAs in SM libraries. **d** Size distribution of total small RNAs in SC libraries. Data shown were means of three libraries for each treatment. MM, Mo17 inoculated with phosphate buffer; SM, Mo17 inoculated with SCMV; MC, Chang7-2 inoculated with phosphate buffer; SC, Chang7-2 inoculated with SCMV

High-throughput sequencing of small RNAs from maize plants

The expression profiles of vsiRNAs are beneficial for elucidating the components and mechanisms involved in their biogenesis and function. To explore the different roles of vsiRNAs in Chang7-2 and Mo17 after SCMV infection, we generated 12 small RNA libraries from the systemic leaves of plants inoculated with SCMV (SM and SC) or phosphate buffer (MM and MC) with three biological replicates and sequenced libraries using the Illumina Solexa high-throughput sequencing platform (Additional file 1: Table S1). Small RNA reads within 18–36 nt were selected for further analysis and aligned to the SCMV genome in sense and antisense orientations. Results revealed that the majority of vsiRNAs were 21- and 22-nt in length in both SM and SC libraries, accounting for 48.96% and 43.85% of total vsiRNAs in SM libraries and 44.68% and 47.15% in SC libraries, respectively (Fig. 2a). Then, we compared the overall profiles of small RNAs between Mock- and SCMV-inoculated Mo17 and Chang7-2 libraries. Results suggested that levels of 21- and 22-nt small RNAs in SM libraries were about twofold of those in MM libraries, while levels of 24-nt

small RNAs were significantly reduced in SM libraries (Fig. 2b). Further analysis showed that the 21- and 22-nt small RNAs in SM libraries were mainly attributed to the accumulation of vsiRNAs (Fig. 2c). In contrast, the small RNAs of 21-, 22-, and 24-nt in SC libraries only increased by about 10% compared with those in MC libraries (Fig. 2b, d). These findings indicated that higher levels of vsiRNAs were produced in Mo17 infected with SCMV, while fewer vsiRNAs, as well as viral accumulation, were detected in Chang7-2 maize plants, which may be the result of antiviral RNA silencing or a specific interaction between the virus and host.

Characteristics of vsiRNAs in SM and SC libraries

To determine the potential interactions between vsiR-NAs and different ZmAGO complexes, we analyzed the properties of 5′-terminal nucleotides of vsiRNAs in SM and SC libraries. The results showed that A and U were the most abundant nucleotides at the 5′-terminal, each accounting for about 30% of 21- and 22-nt vsiRNAs in both SM and SC libraries, while G was the least abundant, accounting for about 15% (Additional file 2: Figure S1a). The clear preference for A and U as the 5′-terminal

Gao *et al. Phytopathology Research*   (2023) 5:60

Page 5 of 18

nucleotides of vsiRNAs from SCMV implied that they were potentially loaded into ZmAGO1, ZmAGO2, and/ or ZmAGO4 homologs.

To examine the origin of vsiRNAs from SCMV genome, we further analyzed the polarity ratio of vsiR-NAs in SM and SC libraries. Results demonstrated that the accumulations of sense vsiRNAs (65.43% and 53.69%) were higher than that of antisense vsiRNAs (34.57% and 46.31%) (Additional file 2: Figure S1b), indicating that sense strand of SCMV RNA was dominant in the production of vsiRNAs.

To further explore the distribution of vsiRNAs, the 21- and 22-nt vsiRNAs in both SM and SC libraries were aligned with SCMV genome (Fig. 3a, b). The resulting single-nucleotide resolution maps showed that vsiRNAs from both stands were almost continuously but heterogeneously distributed throughout the SCMV genome (Fig. 3b). Further analyses indicated that the numbers and regions of vsiRNA hotspots in SM and SC libraries were similar, with vsiRNAs derived more from the sense strand than from the antisense strand, and the cylindrical inclusion (CI) region contained more hotspots (Fig. 3b). However, compared with that in Mo17, the antisense strand of SCMV genome in Chang7-2 contained more hotspots (Fig. 3b).

To verify the existence of vsiRNAs, ten vsiRNAs from different positions of SCMV genome in SM and SC libraries were selected for semiquantitative RT-PCR validation. The results demonstrated that the selected vsiR-NAs had a higher accumulation in SM but less in the SC libraries (Fig. 3c).

Identification of SCMV-responsive circRNAs, lncRNAs, and mRNAs in maize

To explore the different roles of circRNAs, lncRNAs, and mRNAs in the response of Chang7-2 and Mo17 to SCMV infection and determine the function of predicted target genes of vsiRNAs, we performed RNA sequencing (RNA-seq) using the same samples for small RNA sequencing. We obtained an average of 92.80 million raw reads (ranging from 89.10 to 96.99 million) for each library (Additional file 1: Table S2). There were seven differentially

expressed (DE) circRNAs (five up-regulated, two down-regulated) found in SM vs. MM comparison and eight DEcircRNAs (four up-regulated, four down-regulated) in SC vs. MC comparison (Additional file 1: Table S3, 4). In the SM vs. MM comparison, 58 lncRNAs were up-regulated and 305 lncRNAs were down-regulated, while in the SC vs. MC comparison, only 68 lncRNAs were up-regulated and 44 lncRNAs were down-regulated. Among them, three DElncRNAs were co-expressed, of which *Zm00001d026716_T001* was up-regulated, and *MSTRG.18720.1* and *MSTRG.18787.1* were down-regulated in both comparisons (Additional file 1: Table S5, 6). A total of 4058 DEmRNAs (2672 up-regulated, 1386 down-regulated) in SM vs. MM comparison and 2896 DEmRNAs (1576 up-regulated, 1320 down-regulated) in SC vs. MC comparison were identified. In addition, 320 DEmRNAs were uncovered in both comparisons, including 215 DEmRNAs with similar expression trends and 105 DEmRNAs with opposite expression trends (Additional file 1: Table S7, 8).

Gene Ontology (GO) and Kyoto Encyclopedia of Genes and Genomes (KEGG) analyses of vsiRNA target genes

The vsiRNAs usually have a near-perfect complementarity with their targets to regulate gene expression, which can be used to predict target genes of SCMV-derived vsiRNAs in Mo17 and Chang7-2 plants. Due to the wide variety of identified vsiRNAs, we only selected some abundant vsiRNAs (Additional file 1: Table S9, 10) for further investigation. The results indicated that 565 and 713 genes were predicted as targets of 153 and 161 vsiRNAs in Mo17 and Chang7-2, respectively. GO enrichment and KEGG pathway analysis of differentially expressed genes (DEGs) targeted by vsiRNAs were performed. The results showed that DEGs targeted by vsiRNAs found in the SM vs. MM comparison were mainly enriched in GO terms 'oxidation–reduction process,' 'translation,' 'endoplasmic reticulum,' and 'hydrolase activity' (Fig. 4a and Additional file 1: Table S11). In contrast, DEGs targeted by vsiRNAs in SC vs. MC comparison were mainly annotated to GO terms 'phosphorylation,' 'transferase activity,' 'kinase activity,'

(See figure on next page.)
Fig. 3 Single-nucleotide resolution maps and semiquantitative RT-PCR analysis of vsiRNAs. **a** Schematic diagram of SCMV genome. **b** The single-nucleotide resolution maps of 21- and 22-nt vsiRNAs on SCMV genome in SM and SC libraries. The SCMV genome was arranged along the X-axis with length drawn to scale. vsiRNAs derived from the sense and antisense strand of SCMV genomic RNAs were shown above and below the horizontal line, respectively. The data used to generate the charts were based on the means calculated from three libraries for each treatment. **c** Semiquantitative RT-PCR analysis of vsiRNAs in Mock- and SCMV-inoculated Mo17 and Chang7-2 maize plants. Semiquantitative RT-PCR assays were conducted with three independent biological replicates using Mock- and SCMV-inoculated maize plants. "(+)" indicates vsiRNAs derived from the sense strand of SCMV genomes, and "(−)" indicates the antisense strand. U6 was used as the internal control. MM, Mo17 inoculated with phosphate buffer; SM, Mo17 inoculated with SCMV; MC, Chang7-2 inoculated with phosphate buffer; SC, Chang7-2 inoculated with SCMV
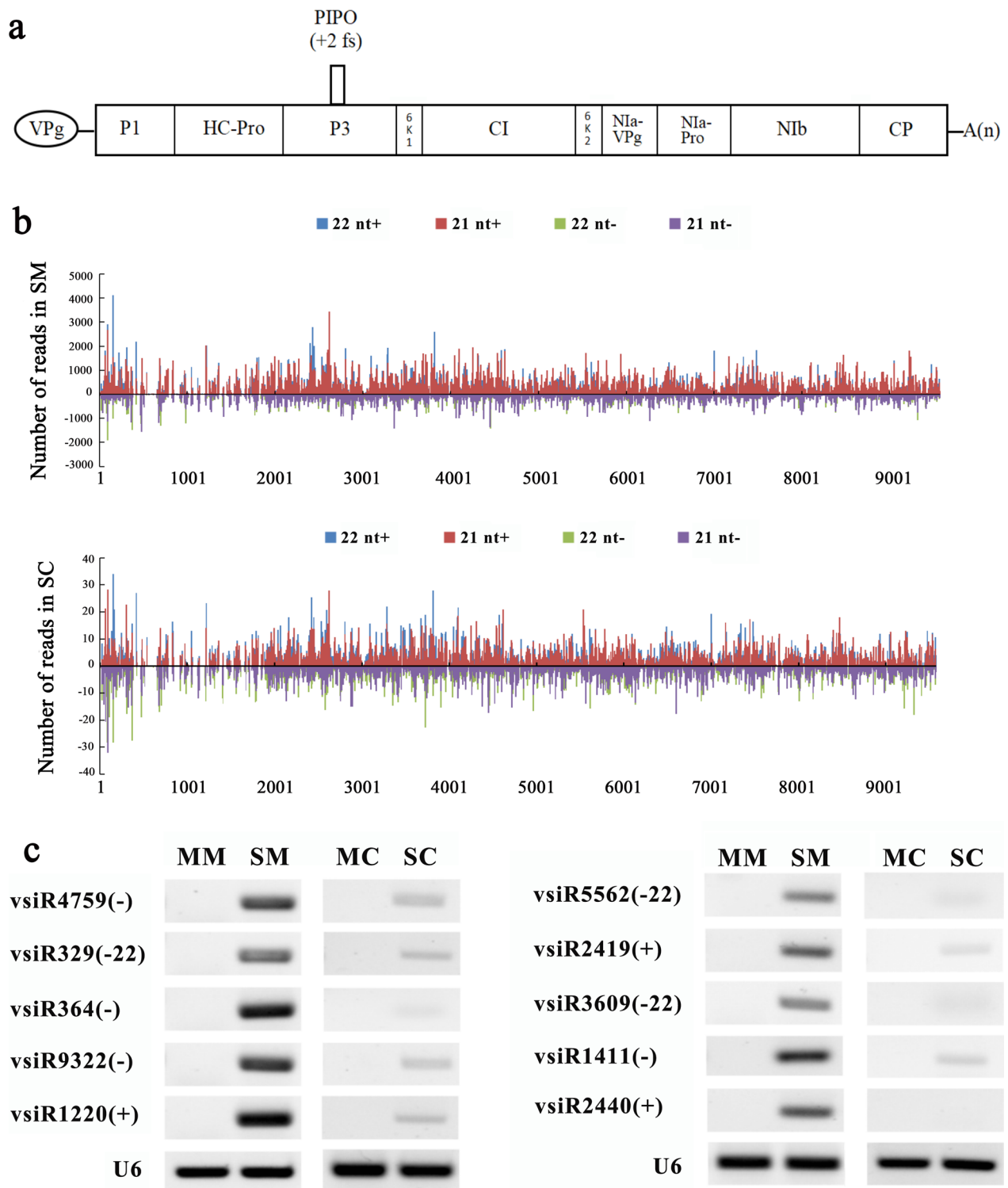
Fig. 3 (See legend on previous page.)

'catalytic activity,' and 'oxidoreductase activity' (Fig. 4b and Additional file 1: Table S12). Results of KEGG pathway analysis indicated that the DEGs targeted by vsiRNAs found in the SM vs. MM comparison were mainly enriched in 'categories proteasome,' 'inositol phosphate metabolism,' 'phenylalanine metabolism,'

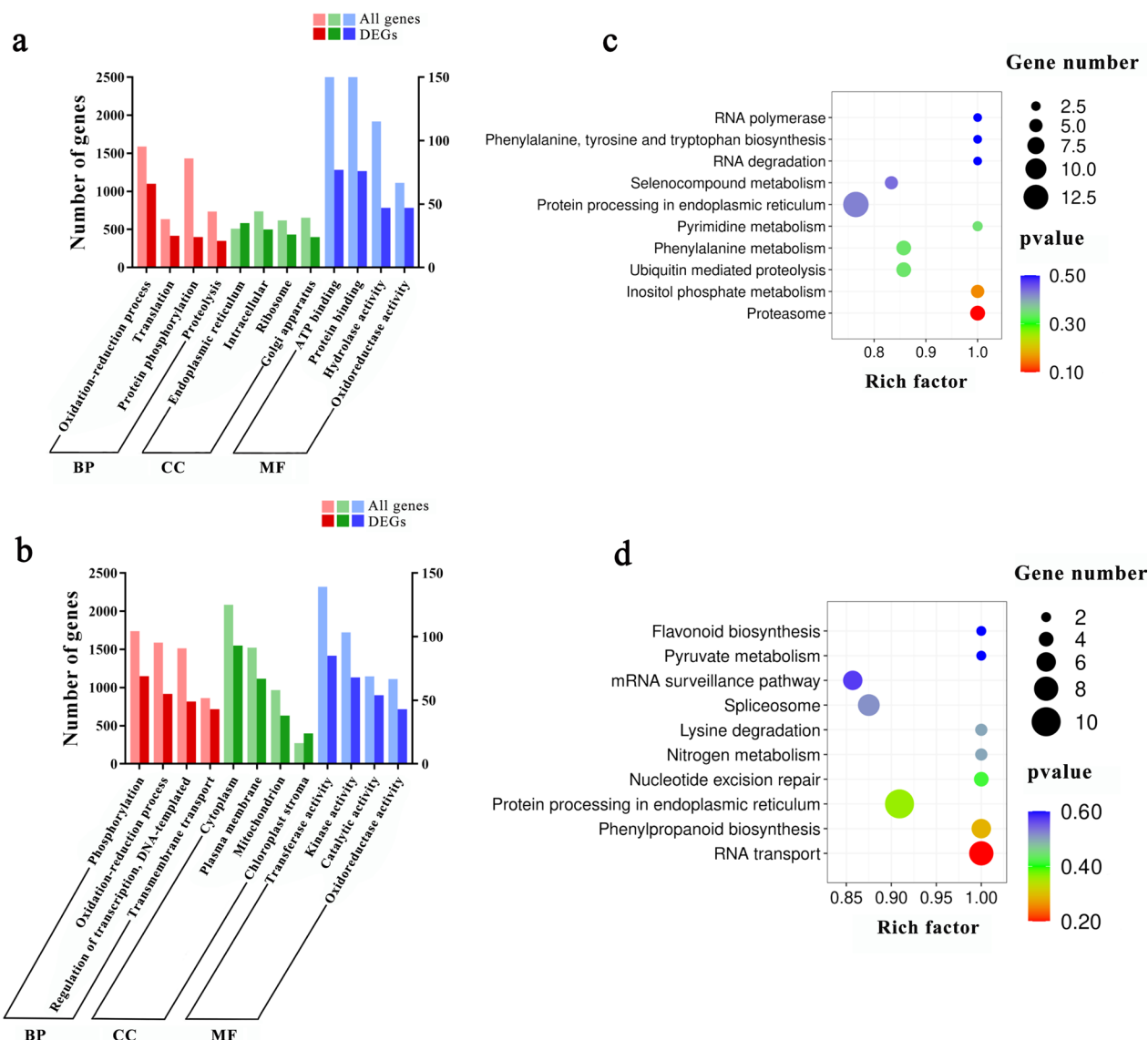Gao *et al. Phytopathology Research*   (2023) 5:60

Page 7 of 18

Fig. 4 GO terms and KEGG pathway enrichment of target transcripts of vsiRNAs in SM and SC libraries. **a, b** GO enrichment analysis results for target transcripts of vsiRNAs in SM and SC libraries, respectively. BP, biological process; CC, cellular component; MF, molecular function. **c, d** KEGG pathway analysis of target transcripts of vsiRNAs in SM and SC libraries, respectively

and 'ubiquitin-mediated proteolysis' (Fig. 4c and Additional file 1: Table S13), while those in the SC vs. MC comparison were enriched in 'RNA transport,' 'phenylpropanoid biosynthesis,' 'protein processing in endoplasmic reticulum,' and 'nitrogen metabolism' (Fig. 4d and Additional file 1: Table S14). The GO and KEGG pathway enrichment analysis results for target genes of the selected ten vsiRNAs are shown in Additional file 1: Table S15. These findings suggested that SCMV-derived vsiRNAs may affect the physiological and biochemical responses by regulating target genes in resistant and susceptible maize materials.

Identification of vsiRNA targets by degradome sequencing

Target identification is essential for understanding the regulatory function of vsiRNAs. We constructed a degradome library using total RNAs derived from MM, MC, SM, and SC to identify target transcripts of vsiRNAs. A total of 10.9 million raw reads were generated. The unique reads were matched to the maize genome and transcriptome data to identify cleavage sites. As a result, 785 vsiRNA-target pairs for 204 vsiRNAs and 706 target transcripts were identified. Some representative cleavage sites are shown as target plots (T-plots) (Fig. 5). The results also showed that a single vsiRNA can act on
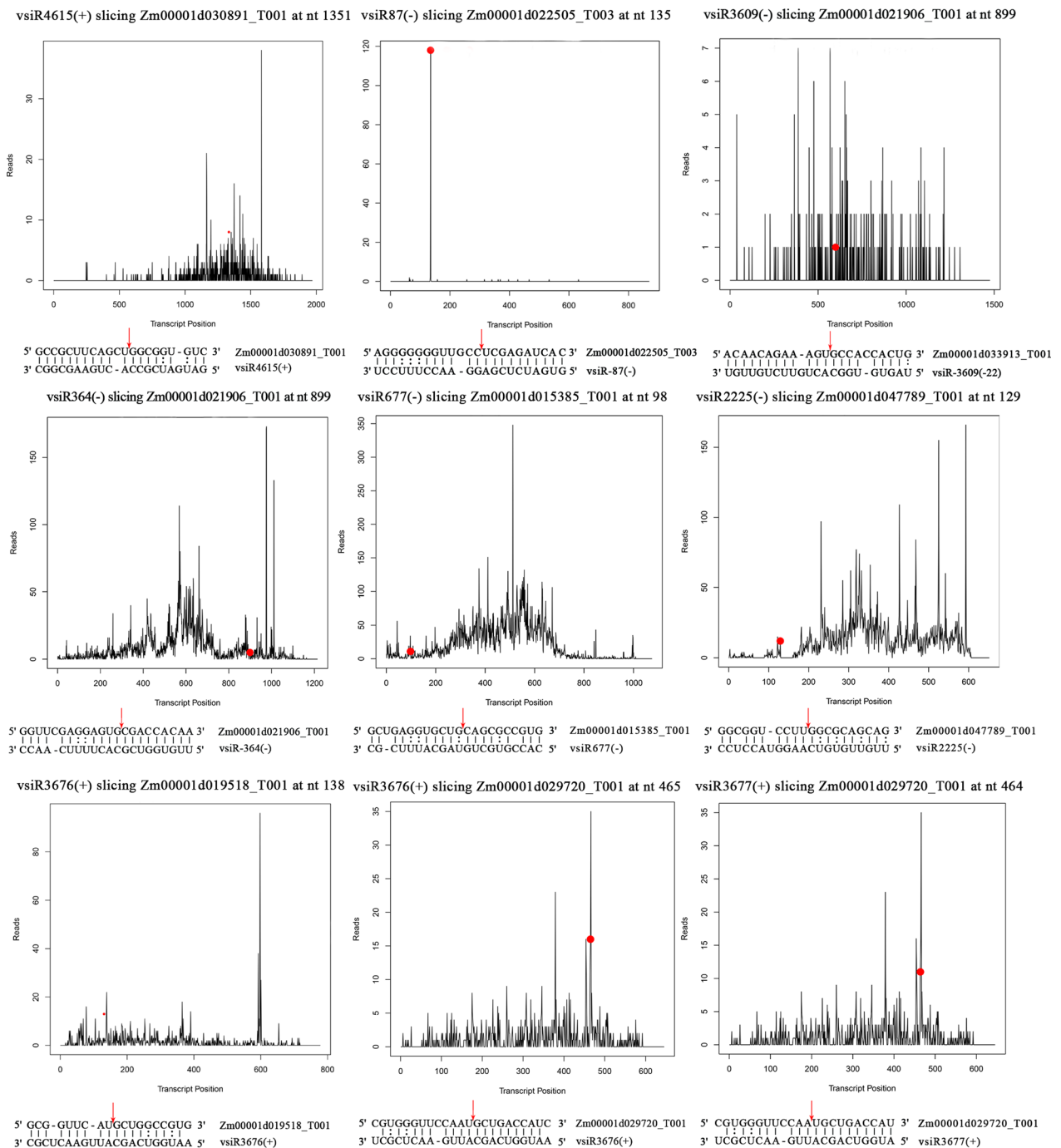
Gao *et al. Phytopathology Research*   (2023) 5:60

Page 8 of 18

Fig. 5 T-plots and alignments of vsiRNA-mRNA pairs validated by degradome sequencing. Target plots for the indicated genes show sequencing signature abundance at the position of target transcripts. The red circles represent cleavage sites of vsiRNAs. The red arrows in the target mRNA sequences represent the cleavage sites identified through degradome sequencing

multiple transcripts, such as vsiR3676(+) can target both *Zm00001d019518_T001* and *Zm00001d029720_T001*. Different vsiRNAs may also synergistically regulate the expression of one transcript, such as *Zm00001d021906_T001* was cleaved by vsiR3609(−) and vsiR364(−), and

Zm00001d029720_T001 cleaved by vsiR3676(+) and vsiR3677(+) (Fig. 5). These findings suggested that there might be a functional redundancy among diverse vsiR-NAs and that a single vsiRNA could cleave multiple transcripts.
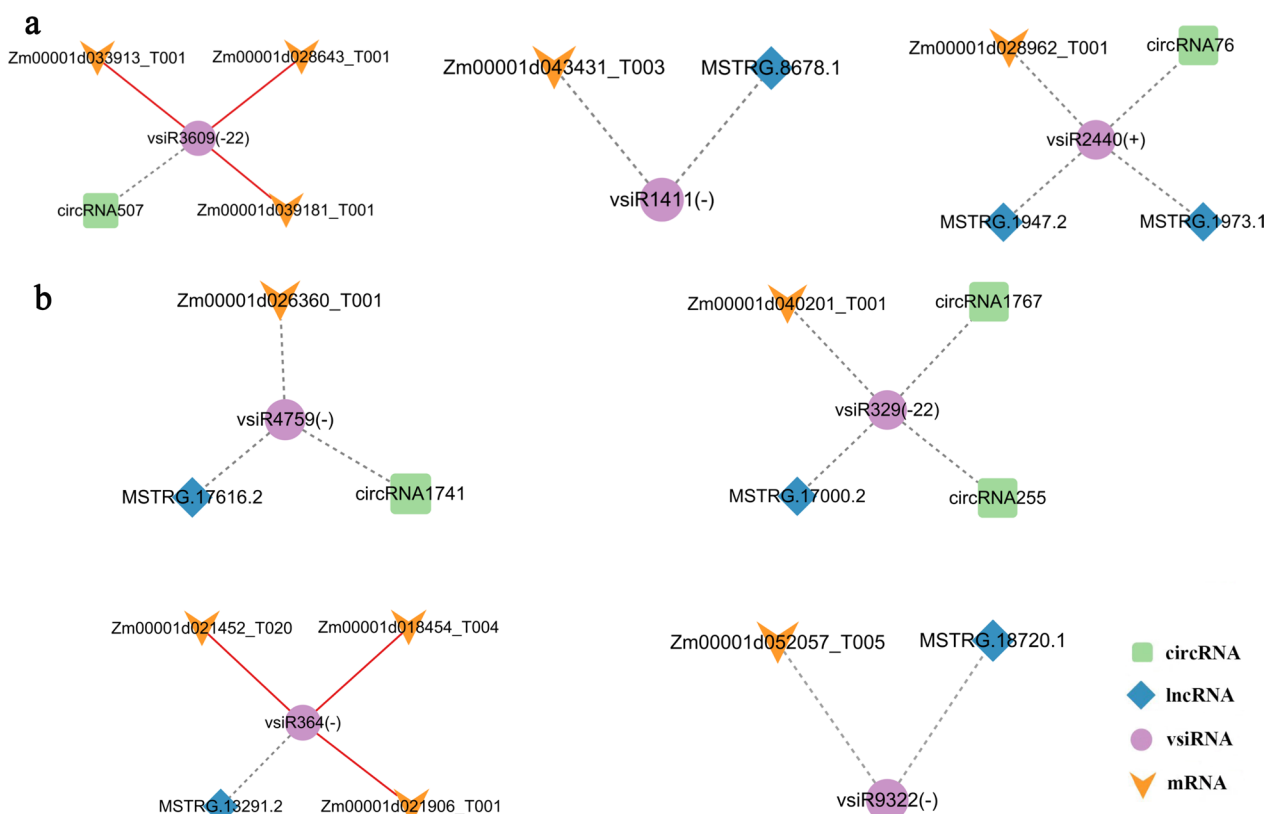
Fig. 6 CeRNA networks constructed with DEcircRNAs, DElncRNAs, vsiRNAs, and DEmRNAs in **a** Chang7-2 and **b** Mo17 plants. Sequences marked with green, blue, purple, and orange symbols represent DEcircRNAs, DElncRNAs, vsiRNAs, and DEmRNAs, respectively. Red solid lines represent regulation verified by degradome sequencing

Construction of vsiRNA-mediated ceRNA regulatory networks

To reveal the relationship between protein-coding RNAs and ncRNAs under SCMV infection, we constructed ceRNA regulatory networks. A total of three DEcircRNAs and 36 DElncRNAs combining with 105 vsiRNAs and competing for the vsiRNA binding sites on 342 DEmRNAs were obtained in Mo17 (Additional file 1: Table S16). However, only three DEcircRNAs and 35 DElncRNAs combining with 23 vsiRNAs that potentially targeted 87 DEmRNAs were identified in Chang7-2 (Additional file 1: Table S17). Among them, five DEcircRNAs, seven DElncRNAs, and 11 DEmRNAs were predicted to target or be targeted by seven vsiRNAs selected in this study (Fig. 6). We found that three vsiRNAs formed two DEcircRNA-vsiRNA, three DElncRNA-vsiRNA, and five vsiRNA-DEmRNA potential interactions in Chang7-2. The coding DEmRNAs of the ceRNA network included alba DNA/RNA-binding protein (*Zm00001d033913_T001*), auxin response factor 11 (*Zm00001d043431_T003*), and WRKY32 (*Zm00001d028962_T001*) (Fig. 6a). Moreover, four

vsiRNAs were found to form three DEcircRNA-vsiRNA, four DElncRNA-vsiRNA, and six DEmRNA-vsiRNA interactions in Mo17. The coding DEmRNAs of the ceRNA network included cyclin-dependent protein kinase (*Zm00001d026360_T001*), protein NRT1/PTR FAMILY 6.1 *(Zm00001d040201_T001*), chlorophyll a-b binding protein (*Zm00001d021906_T001*) and E3 ubiquitin-protein ligase XBAT32 (*Zm00001d052057_T005*) (Fig. 6b). Moreover, RT-PCR and PCR assays were performed to verify the existence of *circRNA507, circRNA1767, circRNA76, circRNA255*, and *circRNA1741* from cDNA and DNA with a total of 10 pairs of divergent and convergent primers. Subsequently, sanger sequencing was performed on the PCR amplification products of divergent primers, further confirming the reverse splicing sites of circRNAs (Additional file 2: Figure S2). The important vsiRNAs and their associated circRNAs, lncRNAs, and mRNAs were summarized and listed in Additional file 1: Table S18. In ceRNA regulatory networks, vsiR3609(-22)-*Zm00001d033913_T001* and vsiR364(-)-*Zm00001d021906_T001* pairs were verified by degradome sequencing (Fig. 5).

Gao *et al. Phytopathology Research*   (2023) 5:60

Page 10 of 18

Validation of the expression of vsiRNA-associated circRNAs, lncRNAs, and mRNAs in Mo17 and Chang7-2 maize plants

To further determine the correlation of ceRNA-vsiRNA-mRNA modules, the expression levels of vsiRNA-associated circRNAs, lncRNAs, and mRNAs were analyzed in Mo17 and Chang7-2 maize plants. The heat map of RNA-seq data shows the expression patterns of circRNAs, lncRNAs, and mRNAs associated with selected vsiRNAs (Fig. 7a). In Chang7-2, the expression levels of *circRNA255*, *MSTRG.13291.2*, *Zm00001d021906_T001*, and *Zm00001d052057_T005* were lower and *circRNA76*, *MSTRG.8678.1*, *Zm00001d026360_T001*, and *Zm00001d040201_T001* were higher than those in Mo17 without SCMV infection (Fig. 7a). The accumulation of these ceRNAs and mRNAs were also determined by quantitative real-time reverse transcription-polymerase chain reaction (qRT-PCR). Among them, the expression levels of *circRNA1741*, *circRNA1767*, *circRNA255*, *circRNA507*, and *circRNA76* were significantly induced by SCMV infection in both Mo17 and Chang7-2. The lncRNAs *MSTRG.17616.2*, *MSTRG.17000.2*, *MSTRG.8678.1*, *MSTRG.1947.2*, and *MSTRG.1973.1* were significantly up-regulated, while *MSTRG.13291.2* and *MSTRG.18720.1* were significantly down-regulated after SCMV infection in Mo17 or Chang7-2. The accumulation of *Zm00001d026360_T001*, *Zm00001d040201_T001*, *Zm00001d033913_T001*, *Zm00001d043431_T003*, and *Zm00001d028962_T001* significantly increased, while that of *Zm00001d021906_T001* and *Zm00001d052057_T005* significantly decreased in Mo17 or Chang7-2 infected with SCMV (Fig. 7b, c). These results were consistent with RNA-seq data (Fig. 7a). Moreover, the expression levels of ceRNAs were positively correlated with mRNAs potentially targeted by vsiRNAs (Figs. 6, 7).

Differential expression of *ZmDCLs*, *ZmAGOs*, and *ZmRDRs* after SCMV infection in Mo17 and Chang7-2

Our results showed that a large amount of 21- and 22-nt vsiRNAs accumulated in Mo17 and Chang7-2 maize plants infected with SCMV (Fig. 2a). To determine the effects of SCMV infection on the RNA silencing pathway, the expression levels of major components in RNA silencing pathway after SCMV infection in Mo17 and Chang7-2 were analyzed by RNA-seq and qRT-PCR. The heat map of RNA-seq data shows the expression pattern of *ZmDCLs*, *ZmAGOs*, and *ZmRDRs* in Mock- and SCMV-inoculated Mo17 and Chang7-2 plants (Fig. 8a). Consistent with the RNA-seq results, the transcript levels of *ZmDCL2* and *ZmDCL3a* significantly increased in SCMV-infected Mo17, whereas the accumulation of *ZmDCL1* and *ZmDCL4* transcripts significantly decreased (Fig. 8b). In addition, SCMV infection

significantly increased the transcript accumulation of *ZmAGO1a*, *ZmAGO1e*, *ZmAGO2*, and *ZmAGO7* in Mo17, while decreased the expressions of *ZmAGO4d*, *ZmAGO10a,* and *ZmAGO10b* (Fig. 8c). The expression levels of *ZmDCL1*, *ZmDCL2*, *ZmDCL3a*, and *ZmDCL4* were significantly increased in SCMV-infected Chang7-2 (Fig. 8d). Similarly, the virus infection significantly increased the transcript accumulation of *ZmAGO1b*, *ZmAGO1e*, and *ZmAGO4d* but decreased that of *ZmAGO4a* in Chang7-2 (Fig. 8e). However, the expression levels of *ZmRDRs* were unchanged after SCMV infection in both Mo17 and Chang7-2 plants (Fig. 8a, f, g). Notably, *ZmDCL2*, *ZmDCL3a,* and *ZmAGO1e* showed similar expression patterns in Mo17 and Chang7-2 plants, whereas for *ZmDCL1*, *ZmDCL4,* and *ZmAGO4d*, opposite patterns of expression were observed in Mo17 and Chang7-2 plants (Fig. 8), suggesting diverse responses of host RNA silencing pathway to SCMV infection in maize resistant and susceptible inbred lines. In conclusion, the expression levels of relevant components in the antiviral RNA silencing pathway in Mo17 and Chang7-2 were significantly affected by SCMV infection, indicating distinct mechanisms underlying interactions of SCMV with resistant and susceptible maize inbred lines.

Discussion

RNA silencing is a small RNA-mediated gene regulation mechanism in eukaryotes, which plays an essential role in plant antiviral responses (Pumplin and Voinnet 2013). In this study, we analyzed the characteristics of vsiRNAs from SCMV in Chang7-2 and Mo17 inbred lines based on high-throughput sequencing and investigated the ceRNA-vsiRNA-mRNA networks to explore the mechanisms mediating the interaction between SCMV and maize plants.

The vsiRNAs produced by DCL4 and DCL2 in plants infected with a positive-strand RNA virus are predominately 21- and 22-nt in length (Fusaro et al. 2006; Donaire et al. 2008). Our study revealed that in SCMV-infected Mo17 plants, 21-nt vsiRNAs were the most abundant species, and 22-nt vsiRNAs accumulated to the highest level in SCMV-infected Chang7-2 plants (Fig. 2a). These results indicated that ZmDCL2 and ZmDCL4 might play different roles in response to SCMV infection in resistant and susceptible inbred lines. Moreover, *ZmDCL2* was up-regulated in SCMV-infected Chang7-2 and Mo17 plants (Fig. 8b, c), confirming its role in antiviral responses and vsiRNA production. However, despite the presence of a large amount of 21-nt vsiRNAs (Fig. 2a), the expression of *ZmDCL4* was reduced in SCMV-infected Mo17 plants (Fig. 8b), which was consistent with previous results observed in SCMV-infected Zong 31 and B73 maize plants (Xia et al. 2014, 2016). However, the accumulation
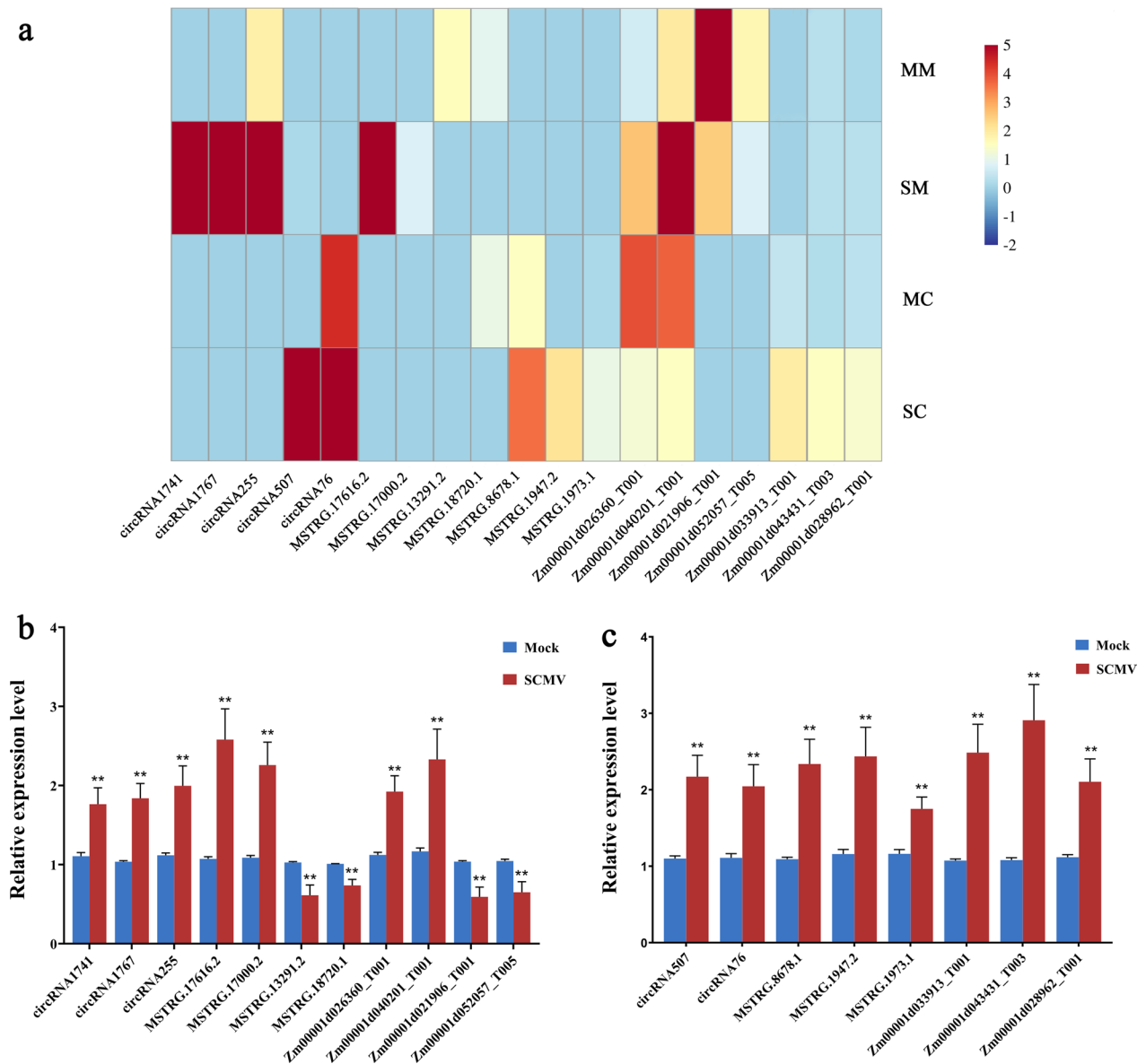
Fig. 7 Expression pattern of vsiRNA-associated circRNAs, lncRNAs, and mRNAs. **a** Heat map of vsiRNA-associated circRNAs, lncRNAs, and mRNAs in Mock- or SCMV-inoculated Mo17 and Chang7-2 libraries. **b** Expression levels of vsiRNA-associated circRNAs, lncRNAs, and mRNAs after SCMV infection in Mo17. **c** Expression levels of vsiRNA-associated circRNAs, lncRNAs, and mRNAs after SCMV infection in Chang7-2. Three independent experiments were conducted with 3 biological replicates. Bars stand for ± SD. Double asterisks indicate *P* < 0.01

(See figure on next page.)
Fig. 8 Expression patterns of *ZmDCLs*, *ZmAGOs*, and *ZmRDRs*. **a** Heat map of *ZmDCLs*, *ZmAGOs*, and *ZmRDRs* in Mock- and SCMV-inoculated Mo17 and Chang7-2 plants. **b, d, f** Relative levels of maize *ZmDCLs, ZmAGOs,* and *ZmRDRs* gene transcripts in Mock- and SCMV-inoculated Mo17 plants. **c, e, g** Relative levels of maize *ZmDCLs, ZmAGOs,* and *ZmRDRs* gene transcripts in Mock- and SCMV-inoculated Chang7-2 plants. The relative expression levels were determined by qRT-PCR assay of samples collected at 9 dpi. Three independent experiments were conducted with three biological replicates each. *ZmUBI* (XM_008647047) was used as an internal control. Data were analyzed using a student *t*-test. Data shown are grand means ± SD. The significance of differences is indicated by single (*P* < 0.05) or double (*P* < 0.01) asterisks
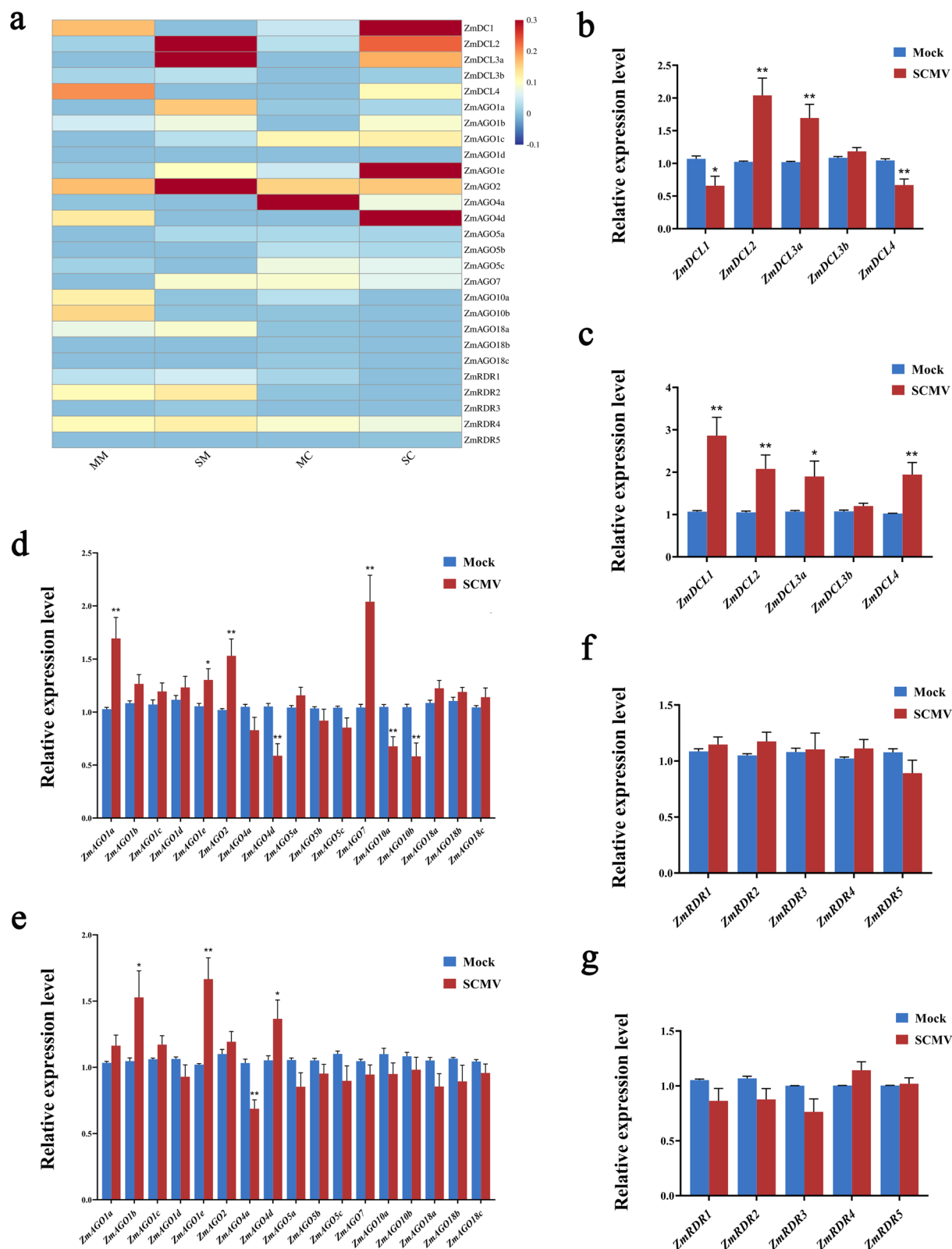
Fig. 8 (See legend on previous page.)

Gao *et al. Phytopathology Research*   (2023) 5:60

Page 13 of 18

of *ZmDCL4* was induced by SCMV infection in Chang7-2 plants, suggesting that ZmDCL4, probably a main component of the RNA silencing pathway, was activated to combat viral infection in the resistant maize inbred line. Interestingly, the accumulation of *ZmDCL2* increased in both resistant and susceptible maize inbred lines, indicating that the induction of *ZmDCL2* is probably a typical response of host plants in antiviral RNA silencing.

Previous studies have shown that the recruitment of vsiRNAs by different AGO complexes is dictated by their 5′-terminal nucleotides (Mi et al. 2008). Our results showed that the proportion of vsiRNAs with a 5′-terminal U was higher in both resistant and susceptible maize inbred lines after SCMV infection (Additional file 2: Figure S1a), which would be mainly loaded into ZmAGO1 that has been reported vital for defense against plant viruses (Harvey et al. 2011). AGO2 and AGO4 are involved in antiviral defense against TBSV and CMV in *N. benthamiana*, respectively (Scholthof et al. 2011; Hamera et al. 2012). This study showed that the 5′-terminal nucleotide of SCMV-derived vsiRNAs has a clear preference for A (Additional file 2: Figure S1a), suggesting a higher binding affinity for AGO2 and/or AGO4 homologues (Donaire et al. 2009). However, the accumulation of *ZmAGO2* increased in Mo17 while unchanged in Chang7-2 plants, and *ZmAGO4d* showed an opposite expression pattern (Fig. 8), suggesting that higher levels of viral RNAs may trigger ZmAGO2 to bind the numerous vsiRNAs in susceptible maize inbred line, while ZmAGO4d was induced in resistant maize inbred line, possibly as the primary defense response. These results indicate that SCMV infection affected the accumulation of distinct *ZmAGOs* in Chang7-2 and Mo17 plants (Fig. 8d, e), suggesting that ZmAGOs play different roles in antiviral defenses in resistant and susceptible maize materials, and the detailed mechanisms still need to be unraveled.

We have found significant differences in the expression levels of *ZmDCLs*, *ZmAGOs*, and *ZmRDRs* in Chang7-2 and Mo17 plants without the SCMV infection. For example, in Chang7-2 plants, the expression levels of *ZmDCL1*, *ZmDCL4*, and *ZmRDR2* were lower, and *ZmAGO4a* and *ZmAGO7* were higher than those in Mo17 (Fig. 8a). After SCMV infection, the expression levels of major components in RNA silencing pathway in resistant and susceptible inbred lines were also diversified (Fig. 8a–e). The accumulations of *ZmDCL1*, *ZmDCL4*, and *ZmAGO4d* were induced in Chang7-2 but decreased in Mo17 after SCMV infection. The expression of *ZmAGO1b* did not change in Mo17 but was significantly up-regulated in Chang7-2 in response to SCMV infection. Although *ZmAGO1e* was up-regulated in both Mo17 and Chang7-2 plants after SCMV infection, it

increased considerably more in Chang7-2. These differentially expressed *ZmDCLs* and *ZmAGOs* probably play essential roles in the resistance of Chang7-2 plants to SCMV infection.

The anti-SCMV processes in plants involve multiple genes and reaction components. Although many studies have demonstrated the roles of ceRNAs in the maintenance of plant response to stresses (Salmena et al. 2011; Song et al. 2021), SCMV-responsive ceRNA regulatory network (ceRNA-vsiRNA-mRNA) in maize has not been extensively constructed. This study identified multiple SCMV-responsive ceRNA networks in Mo17 and Chang7-2 (Fig. 6a, b) plants, advancing the understanding of the role of vsiRNA regulatory pathways in SCMV pathogenesis and plant-virus interactions.

Rice protein OsAlba1 improves plant tolerance to various environmental stress factors under water deficit conditions (Choudhary et al. 2009). Our results showed that the induction of *circRNA507*, a sponge to bind vsiR3609(-22), up-regulated the expression of *Zm00001d033913_T001* (Alba DNA/RNA-binding protein, ZmAlba) that is potentially targeted by vsiR3609(-22) in Chang7-2 plants (Figs. 6a and 7a, c). ARFs play vital roles in various auxin signal-mediated biological processes. The mutants of *osarf11* or *osarf5* enhance the resistance, and *osarf12* or *osarf16* reduce the resistance to RDV in rice (Qin et al. 2020). In this study, *Zm00001d043431_T003* (auxin response factor 11, ZmARF11) was up-regulated by vsiR1411(-)-mediated lncRNA *MSTRG.8678.1* after SCMV infection in Chang7-2 (Figs. 6a and 7a, c). The transcription factor WRKY32 can affect tomato fruit color by regulating *YELLOW FRUITED-TOMATO 1* (Zhao et al. 2021). A previous report demonstrated that *Arabidopsis* transcription factor WRKY55 positively regulates the accumulation of ROS and salicylic acid (SA), thereby controlling leaf senescence and resistance to *Pseudomonas syringae* (Wang et al. 2020). Moreover, *OsWRKY62*, *OsWRKY28*, *OsWRKY71*, and *OsWRKY76* can modulate rice innate immunity (Peng et al. 2010). Here, we found that *circRNA76*, lncRNA *MSTRG.1973.1*, and lncRNA *MSTRG.1947.2* might function as SCMV-responsive ceRNAs, which acted as vsiRNA sponges by binding to vsiR2440(+) and up-regulated the expression of *Zm00001d028962_T001* (WRKY-transcription factor 32, ZmWRKY32) in Chang7-2 (Figs. 6a and 7a, c). These results suggested that specific ceRNAs might act as sponges to bind to vsiRNAs, which regulate the expression of target genes involved in the resistance of Chang7-2 to SCMV infection.

It has been reported that *Arabidopsis cdkc;2 cyct1;5* double mutants were highly resistant to cauliflower mosaic virus (CaMV) (Cui et al. 2007). In *Arabidopsis*, the *cdk8* mutant shows enhanced resistance to *Botrytis*

Gao *et al. Phytopathology Research*   (2023) 5:60

Page 14 of 18

cinerea (Zhu et al. 2014). In this study, the up-regulated *circRNA1741* and lncRNA *MSTRG.17616.2* induced the expression of *Zm00001d026360_T001* (cyclin-dependent protein kinase, ZmCDK) by binding to vsiR4759(-) in Mo17 plants (Figs. 6b and 7a, b). Numerous studies have demonstrated that proteins in the NPF family can transport hormone substrates such as ABA and GA (Chiba et al. 2015). AtNPF5.2 is induced by biotic and abiotic stresses and is involved in plant defense against bacterial pathogens in *Arabidopsis* (Karim et al. 2007). Here, we found that induction of *circRNA1767, cir-cRNA255*, and lncRNA *MSTRG.17000.2* might up-regulate the expression levels of *Zm00001d040201_T001* (protein NRT1/ PTR FAMILY 6.1, ZmNPF6.1) by binding to vsiR329(-22) in Mo17 (Figs. 6b and 7a, b). It has been reported that the leaf yellowing symptom may be caused by the degradation of chlorophyll and the decrease of gene expression levels of major apoproteins in light-harvesting complex II in African cassava mosaic virus (ACMV)-infected cassava plants (Liu et al. 2014). Our data showed that the vsiR364(-)-mediated lncRNA *MSTRG.13291.2* decreased and, in turn, down-regulated the expression of *Zm00001d021906_T001* (Light-harvesting chlorophyll a/b-binding, ZmLHC) in Mo17, which might be involved in the manifestation of mosaic symptom caused by SCMV infection. Mutation of *xbat32* increased plant sensitivity to salt stress during germination and early seedling growth (Prasad and Stone 2010). Our results show that decreased vsiR9322(-)-mediated lncRNA *MSTRG.18720.1* down-regulated the expression of *Zm00001d052057_T005* (E3 ubiquitin-protein ligase ZmXBAT32) in Mo17 (Figs. 6b and 7a, b). These results suggest that ceRNAs may regulate the expression levels of *ZmCDK, ZmNPF6.1, ZmLHC,* and *ZmXBAT32* by binding to vsiRNAs, thereby enhancing Mo17 susceptibility to SCMV infection.

Among ceRNA-vsiRNA-mRNA networks, the expression levels of *circRNA255, MSTRG.13291.2, Zm00001d021906_ T001*, and *Zm00001d052057_T005* in Chang7-2 were lower, while *circRNA76, MSTRG.8678.1, Zm00001d026360_T001*, and *Zm00001d040201_T001* were higher than those in Mo17 without SCMV infection (Fig. 7a). Among the networks *circRNA507-vsiR3609(-22)-Zm00001d033913_T001, MSTRG.8678.1-vsiR1411(-)-Zm00001d043431_T003*, and *circRNA76/MSTRG.1947.2/MSTRG.1973.1-vsiR2440(+)-Zm00001d028962_T001*, ceRNAs, and mRNAs were all significantly induced by SCMV infection in Chang7-2. In *circRNA1741/MSTRG.17616.2-vsiR4759(-)-Zm00001d026360_ T001, circRNA1767/circRNA255/MSTRG.17000.2-vsiR329 (-22)-Zm00001d040201_T001, MSTRG.13291.2-vsiR364(-)-Zm00001d021906_T001*, and *MSTRG.18720.1-vsiR9322(-)-Zm00001d052057_T005* modules, *MSTRG.13291.2,*

MSTRG.18720.1, Zm00001d021906_T001, and *Zm000 01d052057_T005* were significantly decreased, while other ceRNAs and mRNAs were significantly increased after SCMV infection in Mo17. The difference in the expression levels of ceRNAs and mRNAs in Mo17 and Chang7-2 ceRNA-vsiRNA-mRNA networks before and after SCMV infection may be one of the main factors that makes Chang7-2 more resistant to SCMV.

However, other resistance mechanisms in addition to RNA silencing may exist in Chang7-2 plants, such as specific resistance genes, RNA decoy, immune responses, production and accumulation of pathogenesis-related proteins, and ROS burst, which can inhibit the viral multiplication and result in less accumulation of SCMV RNAs and vsiRNAs in Chang7-2 at 10 dpi. The mechanisms underlying the resistance of Chang7-2 to SCMV infection need to be further investigated.

Conclusions

In this study, we performed whole-transcriptome RNA-seq and degradome sequencing to investigate the profiles of SCMV-derived vsiRNAs and construct ceRNA-vsiRNA-mRNA modules in resistant and susceptible maize inbred lines. The characteristics of vsiRNAs were obtained, and the targets of vsiRNAs were predicted and annotated functionally. The ceRNA networks in SCMV-infected Chang7-2 and Mo17 plants were constructed, of which the specific circRNAs and lncRNAs may play important roles as ceRNAs in response to SCMV infection. The transcripts of *ZmDCLs, ZmAGOs,* and *ZmRDRs*, associated with the production and function of vsiRNAs, were differentially expressed in resistant and susceptible maize plants after SCMV infection. These findings highlight an essential role of the ceRNA-vsiRNA-mRNA network in the interaction between SCMV and resistant/susceptible maize plants, and provide new clues to reveal the mechanism underlying the pathogenesis of SCMV.

Methods

Plant materials and virus inoculation

The maize (*Zea mays* L.) inbred lines Chang7-2 and Mo17 were grown in growth chambers (28℃, 16 h day and 22℃, 8 h night cycles). The source of SCMV (GenBank: AY042184.1) was generously provided by Professor Zaifeng Fan (China Agricultural University, Beijing, China) and stored at − 80℃. The crude extracts of maize leaves infected with SCMV were prepared by mixing 0.01 M phosphate buffer solution (0.01 M KH_2PO_4: 0.01 M Na_2HPO_4=49: 51 (V/V), pH 7.0) at a ratio of 1:10 (W/V). The crude extracts were inoculated on the second leaves of six-day-old maize seedlings, and

Gao *et al. Phytopathology Research*   (2023) 5:60

Page 15 of 18

buffer-inoculated plants were used as control. At 10 dpi, the systemic leaves from Mock (MM, MC) and SCMV (SM, SC) treated maize plants were collected. Leaf samples from at least 15 maize seedlings were collected for RNA extraction in each treatment.

Viral accumulation and circRNA validation

Samples were collected from the first systemic leaves of treated Mo17 and Chang7-2 plants at 10 dpi to detect the accumulation of viral RNAs, proteins, and existence of circRNAs. Total RNA, protein, and genomic DNA were extracted using TRIzol Reagent (Vazyme, Nanjing, China), Plant Protein Extraction Kit (Beyotime Biotechnology, Shanghai, China), and Genomic DNA Purification Kit (Sangon, Shanghai, China), respectively. The same amount of cDNA was used for semiquantitative RT-PCR assay, and the accumulation of viral RNA was detected under different amplification cycles. The expression of the *ZmUBI* (XM_008647047) gene served as an internal control. In western blot assays, SCMV CP polyclonal antibody (LV BAO, Chengdu, China) was used to detect the viral protein accumulation. The SCMV CP levels were quantified using ImageJ software (Schneider et al. 2012).

RNA extraction and library construction for RNA sequencing

Total RNA was isolated from the systemic leaves of treated plant samples using TRIzol (Invitrogen, CA, USA) according to the protocol of the manufacturer for qRT-PCR, whole-transcriptome RNA sequencing, and degradome sequencing. To ensure the purity and integrity of the isolated RNA, Bioanalyzer 2100 and an RNA 6000 Nano LabChip Kit (Agilent, CA, USA) were used for RNA quality control.

For whole-transcriptome RNA sequencing, samples of three biological replicates in each group, including Mo17-Mock (MM), Mo17-SCMV (SM), Chang7-2-Mock (MC), and Chang7-2-SCMV (SC), were used to construct 24 libraries. For small RNA sequencing, 12 libraries were generated using TruSeq Small RNA Sample Prep Kits (Illumina, San Diego, USA). In brief, T4 RNA ligase was used to ligate the small RNAs with 3′ and 5′ adapters followed by reverse transcription into cDNAs. The cDNAs were amplified by PCR and the products were purified by polyacrylamide gels. The small RNA sequencing was performed on the Illumina Hiseq 2500 platform (LC Bio, Hangzhou, China).

For circRNA, lncRNA, and mRNA sequencing, ribosomal RNA was depleted from each RNA sample using an Epicentre Ribo-Zero Gold Kit (Illumina, San Diego, USA). After purification, RNA fractions were fragmented into small pieces using divalent cations under a high temperature. Then, the cleaved RNA fragments were reverse transcribed according to the protocol of mRNA sequencing sample preparation kit (Illumina, San Diego, USA) to generate the final cDNA library. The average insert size of the final cDNA library was 300 bp (± 50 bp). Finally, the paired-end sequencing was performed on an Illumina Novaseq™ 6000 (LC Bio, Hangzhou, China).

The original data of RNA sequencing (BioProject: GSE233952) and small RNA sequencing (BioProject: PRJNA978581) have been uploaded to National Center for Biotechnology Information (NCBI) database.

Read mapping and transcriptome assembly

The raw data of whole-transcriptome RNA sequencing were processed using SOAPnuke v1.5.2 (Chen et al. 2018), and sequence quality was verified with FastQC (http://www.bioinformatics.babraham.ac.uk/projects/fastqc/). For small RNA sequencing data, clean reads from each sample were screened in a range of length (18–36 nt). Next, these small RNA sequences were mapped to SCMV genome (Accession number: AY042184), and only those sequences that were identical or complementary to the viral genome sequences within two mismatches were identified as vsiRNAs. For RNA sequencing data, clean reads were mapped to B73 reference genome (ftp://ftp.ensemblgenomes.org/pub/release-45/plants/fasta/zea_mays/dna/, B73_RefGen_v4) using HISAT2 software (http://ccb.jhu.edu/software/hisat2/index.shtml). String-Tie v1.3.0 was used to assemble the mapped reads of each sample (Pertea et al. 2015).

Degradome library construction and sequencing analysis

Total RNA from both treatment and control groups was pooled together to prepare the degradome library. The process of library construction was as follows: (a) mRNA fragments with poly (A) sequences were specifically captured with poly (T) magnetic beads; (b) 5′ RNA adapters were ligated to RNAs containing 5′ monophosphates; (c) The ligated products were purified and reverse-transcribed into cDNAs using biotinylated random primers; (d) The cDNAs were amplified by PCR to construct the degradome libraries; (e) Single-end (36 bp) sequencing was then performed on an Illumina Hiseq 2500 (LC Bio, Hangzhou, China). The original data of degradome sequencing (BioProject: GSE234274) have been uploaded to NCBI database.

The raw reads were processed using ACGT101-DEG (LC Sciences, Houston, Texas, USA) and potential siRNA editing sites were identified using the small RNA sequencing data by CleaveLand4 software (Addo-Quaye

et al. 2009). Thereafter, based on the characteristics and abundance of maize RNA sequencing data, T-plots were established for high efficiency analysis of potential siRNA targets.

GO and KEGG pathway analysis

The predicted target genes of vsiRNAs were aligned based on BLAST (http://blast.ncbi.nlm.nih.gov/). GO analysis was performed to construct annotations of vsiRNA targets using AgriGO v2.0 (Tian et al. 2017). KEGG pathway analysis was implemented to understand the function among targets of vsiRNA by KOBAS 2.0 (Xie et al. 2011). The threshold of significant GO terms and KEGG pathways was set to $p < 0.05$.

Target gene prediction and visualization of ceRNA regulatory network

To understand the potential molecular functions of the candidate vsiRNAs, according to the ceRNA theory, the interaction of ncRNA-vsiRNA and vsiRNA-mRNA pairs were predicted simultaneously by psRNATarget (Dai and Zhao 2011). The ceRNAs networks regulatory network was visualized using Cytoscape v3.7.2 software (Shannon et al. 2003) to display the potential relationships between circRNAs, lncRNAs, vsiRNAs, and mRNAs.

qRT-PCR analysis

Total RNA was extracted from samples by TRIzol Reagent (Vazyme, Nanjing, China) according to the manufacturer's instructions. About 2 μg of total RNA was reverse-transcribed into cDNA with PrimeScript RT Reagent (TaKaRa, Dalian, China). The qRT-PCR reactions were performed on StepOne plus real time PCR platform (Applied Biosystems, Foster City, USA) using SYBR Green PCR Master Mix (Vazyme, Nanjing, China) as instructed. *ZmUBI* (XM_008647047) gene was used as an internal control, and relative gene expression levels in different samples were calculated by the $2^{-\Delta\Delta CT}$ method (Schefe et al. 2006). All primers were listed in Additional file 1: Table S19.

Abbreviations

AGO	Argonaute
CBB	Coomassie brilliant blue
ceRNA	Competing endogenous RNA
circRNA	Circular RNA
CP	Coat protein
DCL	Dicer-like
DE	Differentially expressed
lncRNA	Long non-coding RNA
MC	Chang7-2 inoculated with phosphate buffer
MM	Mo17 inoculated with phosphate buffer
qRT-PCR	Quantitative real time reverse transcription-polymerase chain reaction
RISC	RNA-induced silencing complex
RT-PCR	Reverse transcription-polymerase chain reaction
SA	Salicylic acid
SC	Chang7-2 inoculated with SCMV
SCMV	Sugarcane mosaic virus
SM	Mo17 inoculated with SCMV
vsiRNA	Virus-derived small interfering RNA

Supplementary Information

The online version contains supplementary material available at https://doi.org/10.1186/s42483-023-00216-7.

Additional file 1: Table S1. Statistical analysis of small RNAs from Mock- and SCMV-inoculated resistant and susceptible maize inbred lines. **Table S2.** Statistical analysis of RNA-seq data from 12 cDNA libraries of maize samples. **Table S3.** The differentially expressed circRNAs in Mo17 plants. **Table S4.** The differentially expressed circRNAs in Chang7-2 plants. **Table S5.** The differentially expressed lncRNAs in Mo17 plants. **Table S6.** The differentially expressed lncRNAs in Chang7-2 plants. **Table S7.** The differentially expressed mRNAs in Mo17 plants. **Table S8.** The differentially expressed mRNAs in Chang7-2 plants. **Table S9.** vsiRNAs with high abundance in SM libraries. **Table S10.** vsiRNAs with high abundance in SC libraries. **Table S11.** GO analysis of target genes of selected vsiRNAs from MM libraries. **Table S12.** GO analysis of target genes of selected vsiRNAs from MC libraries. **Table S13.** KEGG analysis of target genes of selected vsiRNAs from MM libraries. **Table S14.** KEGG analysis of target genes of selected vsiRNAs from MC libraries. **Table S15.** GO terms and KEGG pathways for the target genes of selected 10 vsiRNAs. **Table S16.** The ceRNA networks in Mo17 plants. **Table S17.** The ceRNA networks in Chang7-2 plants. **Table S18.** The important vsiRNAs and their associated circRNAs, lncRNAs and mRNAs. **Table S19.** The primers used in this study.

Additional file 2: Figure S1. Relative frequency of the 5′-terminal nucleotides of vsiRNAs and the distribution of sense and antisense stand vsiRNAs. **Figure S2.** Validation of circRNAs. RT-PCR and PCR assays were conducted with a mixed sample consisting of Mock- and SCMV-inoculated Mo17 and Chang7-2 maize plants.

Author contributions
XG, KH, ZD, and SZ performed the experiments. XG analyzed the data. ZX and YW designed the study. XG wrote the draft manuscript. ZX, YW, MA, and ZW revised the manuscript. All authors read and approved the final manuscript.

Availability of data and materials
The datasets presented in this study have been deposited in the NCBI. The accession number is PRJNA978581, GSE233952, and GSE234274.

Declarations

Ethical approval and consent to participate
Not applicable.

Consent for publication
Not applicable.

Competing interests
The authors declare that they have no competing interests.

References

Addo-Quaye C, Miller W, Axtell MJ. CleaveLand: a pipeline for using degradome data to find cleaved small RNA targets. Bioinformatics. 2009;25:130–1. https://doi.org/10.1093/bioinformatics/btn604.

Baumberger N, Baulcombe DC. *Arabidopsis* ARGONAUTE1 is an RNA Slicer that selectively recruits microRNAs and short interfering RNAs. Proc Natl Acad Sci U S A. 2005;102:11928–33. https://doi.org/10.1073/pnas.0505461102.

Bouché N, Lauressergues D, Gasciolli V, Vaucheret H. An antagonistic function for *Arabidopsis* DCL2 in development and a new function for DCL4 in generating viral siRNAs. EMBO J. 2006;25:3347–56. https://doi.org/10.1038/sj.emboj.7601217.

Carbonell A, Carrington JC. Antiviral roles of plant ARGONAUTES. Curr Opin Plant Biol. 2015;27:111–7. https://doi.org/10.1016/j.pbi.2015.06.013.

Chen Y, Chen Y, Shi C, Huang Z, Zhang Y, Li S, et al. SOAPnuke: a MapReduce acceleration-supported software for integrated quality control and preprocessing of high-throughput sequencing data. Gigascience. 2018;7:1–6. https://doi.org/10.1093/gigascience/gix120.

Chiba Y, Shimizu T, Miyakawa S, Kanno Y, Koshiba T, Kamiya Y, et al. Identification of *Arabidopsis thaliana* NRT1/PTR FAMILY (NPF) proteins capable of transporting plant hormones. J Plant Res. 2015;128:679–86. https://doi.org/10.1007/s10265-015-0710-2.

Choudhary MK, Basu D, Datta A, Chakraborty N, Chakraborty S. Dehydration-responsive nuclear proteome of rice (*Oryza sativa* L.) illustrates protein network, novel regulators of cellular adaptation, and evolutionary perspective. Mol Cell Proteom. 2009;8:1579–98. https://doi.org/10.1074/mcp.M800601-MCP200.

Cui X, Fan B, Scholz J, Chen Z. Roles of *Arabidopsis* cyclin-dependent kinase C complexes in cauliflower mosaic virus infection, plant growth, and development. Plant Cell. 2007;19:1388–402. https://doi.org/10.1105/tpc.107.051375.

Dai X, Zhao PX. psRNATarget: a plant small RNA target analysis server. Nucleic Acids Res. 2011;39:155–9. https://doi.org/10.1093/nar/gkr319.

Ding SW. RNA-based antiviral immunity. Nat Rev Immunol. 2010;10:632–44. https://doi.org/10.1038/nri2824.

Ding S, Voinnet O. Antiviral immunity directed by small RNAs. Cell. 2007;130:413–26. https://doi.org/10.1016/j.cell.2007.07.039.

Donaire L, Barajas D, Martínez-García B, Martínez-Priego L, Pagán I, Llave C. Structural and genetic requirements for the biogenesis of *Tobacco rattle virus*-derived small interfering RNAs. J Virol. 2008;82:5167–77. https://doi.org/10.1128/jvi.00272-08.

Donaire L, Wang Y, Gonzalez-Ibeas D, Mayer KF, Aranda MA, Llave C. Deep-sequencing of plant viral small RNAs reveals effective and widespread targeting of viral genomes. Virology. 2009;392:203–14. https://doi.org/10.1016/j.virol.2009.07.005.

Du Q, Wang K, Zou C, Xu C, Li WX. The PILNCR1-miR399 regulatory module is important for low phosphate tolerance in maize. Plant Physiol. 2018;177:1743–53. https://doi.org/10.1104/pp.18.00034.

Fusaro AF, Matthew L, Smith NA, Curtin SJ, Dedic-Hagan J, Ellacott GA, et al. RNA interference-inducing hairpin RNAs in plants act through the viral defence pathway. EMBO Rep. 2006;7:1168–75. https://doi.org/10.1038/sj.embor.7400837.

Gao R, Liu P, Irwanto N, Loh R, Wong SM. Upregulation of LINC-AP2 is negatively correlated with AP2 gene expression with *Turnip crinkle virus* infection in *Arabidopsis thaliana*. Plant Cell Rep. 2016;35:2257–67. https://doi.org/10.1007/s00299-016-2032-9.

Gore MA, Chia JM, Elshire RJ, Sun Q, Ersoz ES, Hurwitz BL, et al. A first-generation haplotype map of maize. Science. 2009;326:1115–7. https://doi.org/10.1126/science.1177837.

Hamera S, Song X, Su L, Chen X, Fang R. Cucumber mosaic virus suppressor 2b binds to AGO4-related small RNAs and impairs AGO4 activities. Plant J. 2012;69:104–15. https://doi.org/10.1111/j.1365-313X.2011.04774.x.

Harvey JJ, Lewsey MG, Patel K, Westwood J, Heimstädt S, Carr JP, et al. An antiviral defense role of AGO2 in plants. PLoS ONE. 2011;6: e14639. https://doi.org/10.1371/journal.pone.0014639.

Huang X, Li F, Zhang X, Chen J, Wang J, Wei J, et al. A virus-derived small RNA targets the rice transcription factor ROC1 to induce disease-like symptom. Phytopathol Res. 2022;4:7. https://doi.org/10.1186/s42483-022-00112-6.

Jiang J, Zhou X. Maize dwarf mosaic disease in different regions of China is caused by *Sugarcane mosaic virus*. Arch Virol. 2002;147:2437–43. https://doi.org/10.1007/s00705-002-0890-7.

Karim S, Holmström KO, Mandal A, Dahl P, Hohmann S, Brader G, et al. AtPTR3, a wound-induced peptide transporter needed for defence against virulent bacterial pathogens in *Arabidopsis*. Planta. 2007;225:1431–45. https://doi.org/10.1007/s00425-006-0451-5.

Liu J, Yang J, Bi H, Zhang P. Why mosaic? Gene expression profiling of *African cassava mosaic virus*-infected cassava reveals the effect of chlorophyll degradation on symptom development. J Integr Plant Biol. 2014;56:122–32. https://doi.org/10.1111/jipb.12133.

Liu W, Cui J, Luan Y. Overexpression of lncRNA08489 enhances tomato immunity against *Phytophthora infestans* by decoying miR482e-3p. Biochem Biophys Res Commun. 2022;587:36–41. https://doi.org/10.1016/j.bbrc.2021.11.079.

Mi S, Cai T, Hu Y, Chen Y, Hodges E, Ni F, et al. Sorting of small RNAs into *Arabidopsis* Argonaute complexes is directed by the 5′ terminal nucleotide. Cell. 2008;133:116–27. https://doi.org/10.1016/j.cell.2008.02.034.

Peng Y, Bartley LE, Canlas P, Ronald PC. OsWRKY IIa transcription factors modulate rice innate immunity. Rice. 2010;3:36–42. https://doi.org/10.1007/s12284-010-9039-6.

Pertea M, Pertea GM, Antonescu CM, Chang TC, Mendell JT, Salzberg SL. String-Tie enables improved reconstruction of a transcriptome from RNA-seq reads. Nat Biotechnol. 2015;33:290–5. https://doi.org/10.1038/nbt.3122.

Prasad ME, Stone SL. Further analysis of XBAT32, an Arabidopsis RING E3 ligase, involved in ethylene biosynthesis. Plant Signal Behav. 2010;5:1425–9. https://doi.org/10.4161/psb.5.11.13294.

Pumplin N, Voinnet O. RNA silencing suppression by plant pathogens: defence, counter-defence and counter-counter-defence. Nat Rev Microbiol. 2013;11:745–60. https://doi.org/10.1038/nrmicro3120.

Qin Q, Li G, Jin L, Huang Y, Wang Y, Wei C, et al. Auxin response factors (ARFs) differentially regulate rice antiviral immune response against rice dwarf virus. PLoS Pathog. 2020;16: e1009118. https://doi.org/10.1371/journal.ppat.1009118.

Qu F, Ye X, Morris TJ. *Arabidopsis* DRB4, AGO1, AGO7, and RDR6 participate in a DCL4-initiated antiviral RNA silencing pathway negatively regulated by DCL1. Proc Natl Acad Sci U S A. 2008;105:14732–7. https://doi.org/10.1073/pnas.0805760105.

Salmena L, Poliseno L, Tay Y, Kats L, Pandolfi PP. A *ceRNA* hypothesis: the Rosetta Stone of a hidden RNA language? Cell. 2011;146:353–8. https://doi.org/10.1016/j.cell.2011.07.014.

Schefe JH, Lehmann KE, Buschmann IR, Unger T, Funke-Kaiser H. Quantitative real-time RT-PCR data analysis: current concepts and the novel "gene expression's C_T difference" formula. J Mol Med. 2006;84:901–10. https://doi.org/10.1007/s00109-006-0097-6.

Schneider CA, Rasband WS, Eliceiri KW. NIH Image to ImageJ: 25 years of image analysis. Nat Methods. 2012;9:671–5. https://doi.org/10.1038/nmeth.2089.

Scholthof HB, Alvarado VY, Vega-Arreguin JC, Ciomperlik J, Odokonyero D, Brosseau C, et al. Identification of an *ARGONAUTE* for antiviral RNA silencing in *Nicotiana benthamiana*. Plant Physiol. 2011;156:1548–55. https://doi.org/10.1104/pp.111.178764.

Schuck J, Gursinsky T, Pantaleo V, Burgyán J, Behrens SE. AGO/RISC-mediated antiviral RNA silencing in a plant in vitro system. Nucleic Acids Res. 2013;41:5090–103. https://doi.org/10.1093/nar/gkt193.

Shannon P, Markiel A, Ozier O, Baliga NS, Wang JT, Ramage D, et al. Cytoscape: a software environment for integrated models of biomolecular interaction networks. Genome Res. 2003;13:2498–504. https://doi.org/10.1101/gr.1239303.

Shi C, Ingvardsen C, Thümmler F, Melchinger AE, Wenzel G, Lübberstedt T. Identification by suppression subtractive hybridization of genes that are differentially expressed between near-isogenic maize lines in association with sugarcane mosaic virus resistance. Mol Genet Genom. 2005;273:450–61. https://doi.org/10.1007/s00438-004-1103-8.

Shimura H, Pantaleo V, Ishihara T, Myojo N, Inaba J, Sueda K, et al. A viral satellite RNA induces yellow symptoms on tobacco by targeting a gene involved in chlorophyll biosynthesis using the RNA silencing machinery. PLoS Pathog. 2011;7: e1002021. https://doi.org/10.1371/journal.ppat.1002021.

Smith NA, Eamens AL, Wang MB. Viral small interfering RNAs target host genes to mediate disease symptoms in plants. PLoS Pathog. 2011;7: e1002022. https://doi.org/10.1371/journal.ppat.1002022.

Gao *et al. Phytopathology Research*   (2023) 5:60

Page 18 of 18

Song L, Fang Y, Chen L, Wang J, Chen X. Role of non-coding RNAs in plant immunity. Plant Commun. 2021;2: 100180. https://doi.org/10.1016/j.xplc.2021.100180.

Tian T, Liu Y, Yan H, You Q, Yi X, Du Z, et al. AgriGO v2.0: a GO analysis toolkit for the agricultural community. Nucleic Acids Res. 2017;45:122–9. https://doi.org/10.1093/nar/gkx382.

Wang XB, Wu Q, Ito T, Cillo F, Li WX, Chen X, et al. RNAi-mediated viral immunity requires amplification of virus-derived siRNAs in *Arabidopsis thaliana*. Proc Natl Acad Sci U S A. 2010;107:484–9. https://doi.org/10.1073/pnas.0904086107.

Wang Y, Cui X, Yang B, Xu S, Wei X, Zhao P, et al. WRKY55 transcription factor positively regulates leaf senescence and the defense response by modulating the transcription of genes implicated in the biosynthesis of reactive oxygen species and salicylic acid in *Arabidopsis*. Development. 2020. https://doi.org/10.1242/dev.189647.

Wang C, Jiang F, Zhu S. Complex small RNA-mediated regulatory networks between viruses/viroids/satellites and host plants. Virus Res. 2022;311: 198704. https://doi.org/10.1016/j.virusres.2022.198704.

Xia Z, Peng J, Li Y, Chen L, Li S, Zhou T, et al. Characterization of small interfering RNAs derived from *Sugarcane mosaic virus* in infected maize plants by deep sequencing. PLoS ONE. 2014;9: e97013. https://doi.org/10.1371/journal.pone.0097013.

Xia Z, Zhao Z, Chen L, Li M, Zhou T, Deng C, et al. Synergistic infection of two viruses MCMV and SCMV increases the accumulations of both MCMV and MCMV-derived siRNAs in maize. Sci Rep. 2016;6:20520. https://doi.org/10.1038/srep20520.

Xie C, Mao X, Huang J, Ding Y, Wu J, Dong S, et al. KOBAS 2.0: a web server for annotation and identification of enriched pathways and diseases. Nucleic Acids Res. 2011;39:316–22. https://doi.org/10.1093/nar/gkr483.

Yang Y, Liu T, Shen D, Wang J, Ling X, Hu Z, et al. Tomato yellow leaf curl virus intergenic siRNAs target a host long non-coding RNA to modulate disease symptoms. PLoS Pathog. 2019;15: e1007534. https://doi.org/10.1371/journal.ppat.1007534.

Yang J, Zhang T, Li J, Wu N, Wu G, Yang J, et al. *Chinese wheat mosaic virus*-derived vsiRNA-20 can regulate virus infection in wheat through inhibition of vacuolar- (H$^+$)-PPase induced cell death. New Phytol. 2020;226:205–20. https://doi.org/10.1111/nph.16358.

Ye J, Qu J, Zhang JF, Geng YF, Fang RX. A critical domain of the *Cucumber mosaic virus* 2b protein for RNA silencing suppressor activity. FEBS Lett. 2009;583:101–6. https://doi.org/10.1016/j.febslet.2008.11.031.

Zhao W, Li Y, Fan S, Wen T, Wang M, Zhang L, et al. The transcription factor WRKY32 affects tomato fruit colour by regulating *YELLOW FRUITED-TOMATO 1*, a core component of ethylene signal transduction. J Exp Bot. 2021;72:4269–82. https://doi.org/10.1093/jxb/erab113.

Zhu H, Duan CG, Hou WN, Du QS, Lv DQ, Fang RX, et al. Satellite RNA-derived small interfering RNA satsiR-12 targeting the 3′ untranslated region of *Cucumber mosaic virus* triggers viral RNAs for degradation. J Virol. 2011;85:13384–97. https://doi.org/10.1128/jvi.05806-11.

Zhu Y, Schluttenhoffer CM, Wang P, Fu F, Thimmapuram J, Zhu JK, et al. CYCLIN-DEPENDENT KINASE8 differentially regulates plant immunity to fungal pathogens through kinase-dependent and -independent functions in *Arabidopsis*. Plant Cell. 2014;26:4149–70. https://doi.org/10.1105/tpc.114.128611.